Nat. Hazards Earth Syst. Sci. Discuss., https://doi.org/10.5194/nhess-2018-403
Manuscript under review for journal Nat. Hazards Earth Syst. Sci.
Discussion started: 27 March 2019

Natural Hazards and Earth System Sciences
Open Access
Discussions

Drought risk in the Bolivian Altiplano associated with El Niño Southern Oscillation using satellite imagery data

Claudia Canedo-Rosso[1,2], Stefan Hochrainer-Stigler[3], Georg Pflug[3,4], Bruno Condori[5], and Ronny Berndtsson[1,6]

[1]Division of Water Resources Engineering, Lund University, P.O. Box 118, SE-22100 Lund, Sweden
[2] Instituto de Hidráulica e Hidrología, Universidad Mayor de San Andrés, Cotacota 30, La Paz, Bolivia
[3] International Institute for Applied Systems Analysis (IIASA), Schlossplatz 1, A-2361 Laxenburg, Austria
[4] Institute of Statistics and Operations Research, Faculty of Economics, University of Vienna, Oskar-Morgenstern-Platz 1, 1090 Wien, Austria
[5] Instituto Nacional de Innovación Agropecuaria y Forestal (INIAF), Batallón Colorados 24, La Paz, Bolivia.
[6] Center for Middle Eastern Studies, Lund University, P.O. Box 201, SE-22100 Lund, Sweden.

Correspondence to: Claudia Canedo-Rosso (canedo.clau@gmail.com and claudia.canedo_rosso@tvrl.lth.se)

Abstract. Drought is a major natural hazard in the Bolivian Altiplano that causes large losses to farmers, especially during positive ENSO phases. However, empirical data for drought risk estimation purposes are scarce and spatially uneven distributed. Due to these limitations, similar to many other regions in the world, we tested the performance of satellite imagery data for providing precipitation and temperature data. The results show that droughts can be better predicted using a combination of satellite imagery and ground-based available data. Consequently, the satellite climate data were associated with the Normalized Difference Vegetation Index (NDVI) in order to evaluate the crop production variability. Moreover, NDVI was used to target specific drought hotspot regions. Furthermore, during positive ENSO phase (El Niño years), a significant decrease in crop yields can be expected and we indicate areas where losses will be most pronounced. The results can be used for emergency response operations and enable a pro-active approach to disaster risk management against droughts. This includes economic-related and risk reduction strategies such as insurance and irrigation.

Keywords: Drought risk management, agriculture, ENSO, climate variables, NDVI, Quinoa and Potato yield.

1. Introduction

Agricultural production is highly sensitive to weather extremes, including droughts and heat waves. Losses due to such extreme hazardous events pose a significant challenge to farmers as well as governments worldwide (UNISDR, 2015). Worryingly, the scientific community predicts an amplification of these negative impacts due to future climate change (IPCC, 2013). Especially in developing countries such as Bolivia, drought is a major natural hazard and Bolivia has experienced large socio-economic losses in the past due to such events. However, the impacts vary on a seasonal and annual timescale, hazard intensity, and capacity to prevent and respond to droughts (UNISDR, 2009). Regarding the former, the El Niño Southern Oscillation (ENSO) plays an especially important role in several regions of the world, including the Bolivian Altiplano, as it drives losses in agricultural crops, and causes increased food insecurity (Kogan and Guo, 2017). Most important rainfed crops in the region include quinoa and potato (Garcia et al., 2007). Generally speaking, agricultural productivity in the Bolivian Altiplano is low due to adverse weather and poor soil conditions (Garcia et al., 2003). On the other hand, low agricultural production levels can also be associated with the ENSO climate phenomena (Buxton et al., 2013). For this area, droughts are generally driven by the ENSO warm phases (Vicente-Serrano et al., 2015; Garreaud and Aceituno, 2001; Thompson et al., 1984). Previous research has addressed the influence of ENSO on agriculture (e.g. Anderson et al., 2017; Iizumi et al., 2014; Ramirez-Rodrigues et al., 2014). Moreover, Anderson et al. (2017) synthetized published studies on this topic. The studies suggest that a better understanding of the association between ENSO and agriculture could improve the crop management and food security.

In this regard, the Sustainable Development Goals (SDGs) state that priorities for adaptation to climate change include water and agricultural dimensions. These in turn, can be related to extreme natural hazardous phenomena including floods, droughts, and higher temperatures (UN, 2016). The implementation of drought risk management approaches is now seen as fundamental for developing a strategic plan processes and the planning of mitigation policy measures for sustainable development in vulnerable regions, including Latin American countries such as Bolivia (Verbist et al., 2016). To lessen the long-term impacts of these extreme events, the national government in Bolivia has taken several steps, e.g., to allocate budgets for emergency operations to compensate part of the losses, which are usually evaluated ex-post (i.e. after the event). However, based on ENSO forecasting, an El Niño event can be predicted 1 to 7 months ahead (Tippett et al., 2012) and consequently there is also opportunity to implement additional ex-ante policies (i.e. before the event) to reduce societal impacts to droughts, increase preparedness, and generally improve current risk management strategies.

This paper addresses the corresponding question how a risk based approach can be used to determine the potential need of resources during droughts and provide ways forward how to determine hotspot areas where it is most likely that such resources would be needed. One major constraint for developing countries, when it comes to analyse current and future drought occurrences, is the uneven and scarce distribution of weather and crop related ground data. To circumvent this problem we suggest to use rainfall, land surface temperature, and vegetation satellite data so as to have a full coverage (of land area) for drought risk and its spatial distribution in the study area. Furthermore, these data are combined with empirically gauged precipitation, temperature and crop yield data on the ground level to enhance the knowledge and provide consistent relationship between agriculture production and climate variability. Finally, the approach is used to assess drought risk impacts on agriculture associated with ENSO for the Bolivian Altiplano which was found to be significantly important to be considered within any drought risk management strategy. We provide ways forward to tackle these challenges using a risk based approach. The paper is organized as follows, section 2 will present the methodology applied and data used, while section 3 will present the results. Section 4 gives a discussion in regards to risk management strategies and finally, section 4 concludes and provides an outlook to the future.

2. Data Used and Methodology

2.1 Ground data and satellite imagery

Climate-wise, the Altiplano has a pronounced southwest-northeast precipitation gradient (200–900 mm year^{-1}) during the wet season occurring from November to March (Garreaud et al., 2003). Over 60% of total precipitation occur during summer months (DJF) in association with the South American Monsoon (SAM) (see Fig. 1a). Time series of monthly precipitation at 23 locations as well as mean, maximum, and minimum temperature at 11 locations from September 1981 to August 2015 were obtained from the National Service of Meteorology and Hydrology (SENAMHI) of Bolivia (see Table A1). Initially, the available precipitation data set included 65 gauges but only 23 were used as they had less than 10% of missing data (chosen as cut-off point for use in the analysis). Data gaps were filled with mean monthly values from the full dataset.

As already indicated, precipitation and temperature gauge locations are unevenly distributed and mainly concentrated in the northern Bolivian Altiplano. To improve the spatial coverage of rainfall data, monthly quasi-rainfall time series from satellite data were therefore included in our study. The Climate Hazards Group InfraRed Precipitation with station data (CHIRPS) from the quasi-global rainfall dataset was used. CHIRPS represents a 0.05° resolution satellite imagery and is a quasi-global rainfall dataset from 1981 to the near present with a satellite resolution of 0.05° (Funk et al., 2015). The advantage of using CHIRPS is the higher spatial resolution of data, i.e., the resolution of 0.05°, obtained with resampling of TMPA 3B42 (with 0.25° grid cell). The spatial resolution represents a better option for agricultural studies (CHIRPS is described in detailed at http://chg.geog.ucsb.edu/data/chirps/).

Nat. Hazards Earth Syst. Sci. Discuss., https://doi.org/10.5194/nhess-2018-403
Manuscript under review for journal Nat. Hazards Earth Syst. Sci.
Discussion started: 27 March 2019

Natural Hazards and Earth System Sciences
Open Access
Discussions

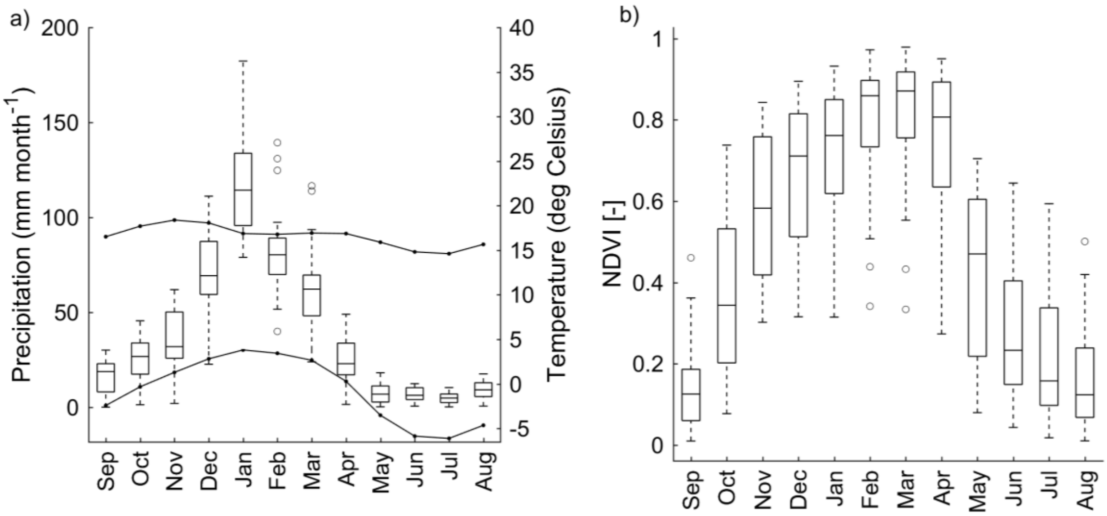

Fig 1. (a) Mean monthly total precipitation and average maximum and minimum temperature from September 1981 to August 2015 of the 23 gauged stations. (b) The mean monthly NDVI at the same spatial locations.

Additionally, monthly mean land surface temperature (LST) was obtained from the Global Historical Climatology Network and the Climate Anomaly Monitoring System (GHCN and CAMS) from the US National Oceanic and Atmospheric Administration (NOAA, https://www.esrl.noaa.gov/psd/data/gridded/data.ghcncams.html). The LST has a resolution of 0.5° and it is conveniently also available during the study period from September 1981 to August 2015.

2.2 Validation of satellite rainfall and temperature products using gauged data

The performance of the satellite products to accurately estimate amount of rainfalls (i.e., to assess rain detection capability) was based on statistical measures including categorical analyses as suggested in the literature (Blacutt et al., 2015; Satgé et al., 2016). The mean error (ME), also called bias, was calculated based on Wilks (2006). Additionally, the Nash-Sutcliffe efficiency (E) coefficient was calculated based on Nash and Sutcliffe (1970). The bias shows the degree of over- or underestimation (Duan et al., 2015), and the E coefficient evaluates the prediction accuracy compared to observations. E equals to one that corresponds to a perfect match between gauge

Nat. Hazards Earth Syst. Sci. Discuss., https://doi.org/10.5194/nhess-2018-403
Manuscript under review for journal Nat. Hazards Earth Syst. Sci.
Discussion started: 27 March 2019

Natural Hazards and Earth System Sciences
Open Access
Discussions

observation and satellite-based estimate and zero indicates that the satellite estimations are as accurate as the mean of observed data. Negative values indicate that the observed mean is better than satellite-based estimate, see Nash and Sutcliffe (1970) for more details. Furthermore, and similar to Blacutt et al. (2015) and Satgé et al. (2016), the Spearman rank correlation was computed to estimate the goodness of fit to observations. To evaluate results, as done in similar studies, correlation coefficients larger or equal to 0.7 with a significance level of 0.01 were considered as reliable (Satgé et al., 2016; Condom et al., 2011).

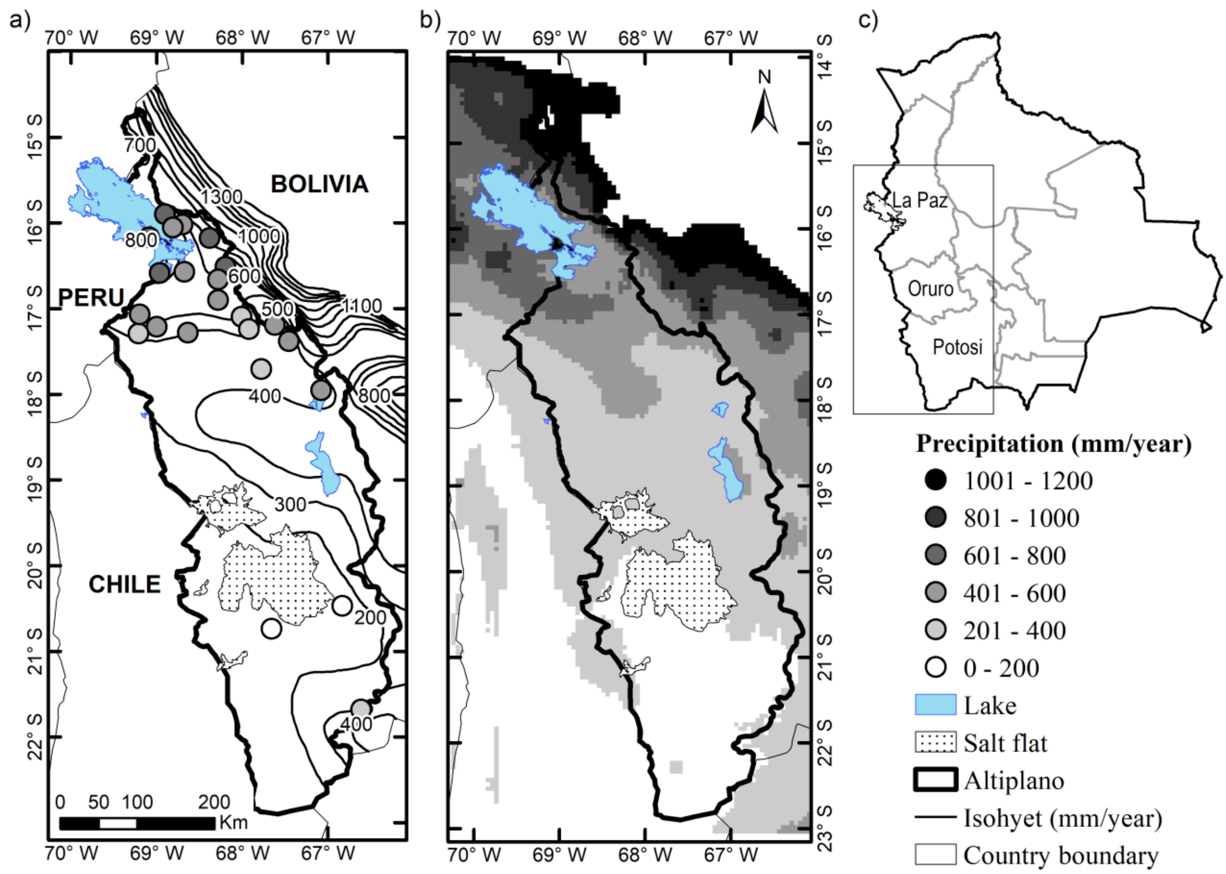

Fig. 2. The mean of the total annual precipitation from September 1981 to August 2015 for: (a) gauged precipitation data (circles) and isohyets (solid line), (b) the CHIRPS satellite rainfall product, and (c) Bolivia, and the major political divisions: La Paz, Oruro and Potosi, where crop yield data is available in the Altiplano.

Two statistical indicators based on a contingency table were computed for the categorical statistics, namely Probability of Detection (POD) and False Alarm Ratio (FAR). The POD indicates which fraction of the observed events was correctly estimated, and FAR indicates the fraction of the predicted events that did not occur (Bartholmes et al., 2009; Ochoa et al., 2014; Satgé et al., 2016). The POD and FAR range from 0 to1, where 1 is a perfect score for POD, and 0 is a perfect score for FAR. The categorical statistic measures were used to evaluate the satellite estimations. Here, the rainfall amounts are considered as discrete values, i.e., rain occurrence or absence. Based on this approach, four scenarios were taken into account: the number of events when the satellite rain estimation and the rain gauge report a rain event (H), when only the satellite reports a rain event but is a false alarm (F), and when only the rain gauge reports a rain event but not the satellite not and therefore is a miss (M).

Besides the precipitation data also satellite temperature data were validated using ground data. The LST was correlated with the mean gauged temperature at the same spatial location. The mean temperature of the gauged data was calculated using the arithmetic mean between the maximum and minimum temperature. The relationship enables to correct the LST with a linear regression equation (Zhou and Wang, 2016). The regression performance was evaluated using the relative ME or bias and the E coefficient.

2.3 Crop yield simulation based on NDVI data

As indicated above, quinoa and potato are the main crops in the Bolivian Altiplano and they are still gaining importance. The quinoa growing season is from September to April and for potato it is from October to March. Yield data from 1981 to 2015 for quinoa and potato were obtained from the Bolivian National Institute of Statistics (INE, https://www.ine.gob.bo) for the administrative regions La Paz, Oruro, and Potosi (Fig. 2). The annual crop yield datasets represent production (t) in relation to area (ha) at regional level. No historical crop yield data on local scales are available yet which is a major limitation for any risk-based approach and needs to be addressed in the future. Nevertheless, we suggest that the coarse distribution of the crop yield data can be improved using the NDVI. Besides improving the crop yield resolution, the NDVI also allows to analyse the variability of vegetation at a monthly time scale. This makes it possible analyse the phenology of the studied crops through to the growth phases. NDVI estimates the vegetation vigour (Ji and Peters, 2003) and crop phenology (Beck et al., 2006). NDVI was assembled from the Advanced Very High Resolution Radiometer (AVHRR) sensors by the Global Inventory Monitoring and Modelling System (GIMMS) at semi-monthly (15 days) time steps with a spatial resolution of 0.08°. NDVI 3g.v1 (third generation GIMMS NDVI from AVHRR sensors) and the data set spans from September 1981 to August 2015. Note, the NDVI is an index that presents a range of values from 0 to 1, bare soil values are

Nat. Hazards Earth Syst. Sci. Discuss., https://doi.org/10.5194/nhess-2018-403
Manuscript under review for journal Nat. Hazards Earth Syst. Sci.
Discussion started: 27 March 2019

Natural Hazards and Earth System Sciences
Open Access
EGU
Discussions

closer to 0, while dense vegetation has values close to 1 (Holben, 1986). NDVI 3g.v1 GIMMS provides information to differentiate valid values from possible errors due to snow, cloud, and interpolation errors. These errors were eliminated from the dataset and replaced with the nearest neighbour value.

Relationships between crop yield and NDVI for agricultural land area of the Altiplano were developed using Spearman's rank correlation, based on a similar approach by Huang et al. (2014). The maximum semi-monthly NDVI of March and April for every year was identified. Only March and April were considered because this period represents the maximum phenological development of quinoa and potato crops. The maximum NDVI of each grid was compared to the annual crop yield at La Paz, Oruro, and Potosi. The NDVI grids and crop yield correlations equal or larger than 0.6 (Spearman correlation, p = 0.05) were considered as adequate for crop yield estimation, and only these grids were considered for further use. As will be discussed further below, a regression approach was applied for selected NDVI grids and corresponding climate variables (precipitation and temperature). In doing so, the agricultural land in the Bolivian Altiplano was delimited based on the land use map for Bolivia developed by Raul Lara Rico from the Ministry of Rural Development and Land of Bolivia in 2010 (geo.gob.bo) using Landsat imagery and ground information at a scale 1:1,000,000.

2.4 Regression of vegetation and climate variables

Only the NDVI grids that properly simulated the crop yield were related to climate variables. Thus, the stepwise regression approach was used to quantify the dependency between vegetation and satellite based climate variables (precipitation and temperature; Eq. 1). The final results presented are a combination of forward and backward selection techniques to increase the robustness of the results. The independent variable considered was the NDVI, and the dependent variables were accumulated precipitation and accumulated degree days (ADD) for the same spatial location. Firstly, the NDVI was related to CHIRPS rainfall datasets. Secondly, the ADD was included in the analysis. For this, only the NDVI grids that better simulated the crop yield of quinoa and potato were used (see section 2.3).

$$NDVI = \beta_0 + \beta_1 accumulated\ precipitation + \beta_2 accumulated\ degree\ days \qquad (1)$$

Both precipitation and temperature were represented as accumulated values (for temperature using the GDD). The mean monthly temperature was multiplied by the number of days of each month to obtain daily values. GDD was computed only considering the months of the growing season for each year. To calculate the ADD, the accumulated value of the Growing Degree Day (GDD) multiplied by the number of days of each month was computed. The GDD is defined as the difference between mean and base temperature. The mean temperature is the arithmetic average between maximum and minimum temperature, and T_b is the minimum threshold or base temperature. Base temperature of potato was 4°C and 3°C for quinoa (Jacobsen and Bach, 1998). If T_b is greater than T_{mean}, then GDD is equal to 0. For the ADD calculation we considered crop phenology, September to April were used to calculate the ADD for quinoa, and from October to April for potato.

For the forward selection, the variables were entered into the model one at a time in an order determined by the strength of their correlation with the criterion variable (only including variables if they are significant on the 5 percent level). The effect of adding each variable was assessed during its entering stage, and variables that did not significantly added to the fit of the model were excluded (Kutner et al., 2004). For backward selection, all predictor variables were entered into the model first. The weakest predictor variable was then removed and the regression fit re-calculated. If this significantly weakened the model then the predictor variable was re-entered, otherwise it was deleted. This procedure was repeated until only useful predictor variables (in a statistical sense, e.g. significant as well as model fit) remained in the model (Rencher, 1995). The results were compared with other results from the literature to check for suitability of results with phenology and weather related dimensions of plants. It should be noted that the cumulative precipitation was calculated for a period of 12 months from September to August of the following year for all locations. The precipitation in the Altiplano shows a marked rainy season from November to March. The highest peak of precipitation is in December and January (Fig. 1a). And, NDVI displays the highest peak in March and April (Fig. 1b). The lag between the max precipitation and max NDVI is reasonable since vegetation requires time to grow (e.g. Shinoda, 1995; Cui and Shi, 2010; Chuai et al., 2013). The accumulated precipitation and NDVI with a lag of two, three, and four month lag was developed for the agricultural area.

2.5 Crop yield relationship with ENSO

The Oceanic Niño Index (ONI) is usually used to identify El Niño (warm) and La Niña (cool) years (http://www.cpc.ncep.noaa.gov/). ONI is the 3-month running mean of Extended Reconstructed Sea Surface Temperature (ERSST v5) anomalies in the El Niño 3.4 region. The El Niño 3.4 anomalies represent the average equatorial SSTs in the equatorial Pacific Ocean (5ºN to 5ºS latitude, and 120º to 170ºW longitude). Five consecutive overlapping three month periods at or above +0.5°C anomaly represent warm events (El Niño), and at or below the -0.5 anomaly cold (La Niña) events. This threshold was further broken down into weak (with a

0.5 to 0.9 SST anomaly), moderate (1.0 to 1.4), and strong (≥ 1.5) events (http://ggweather.com/enso/oni.htm). In our study we considered the categories neutral/moderate (with a 0 to 1.4 SST), strong El Niño (≥ 1.5) and strong La Niña (≤ -1.5) years (Appendix Table A2). The classification considered three consecutive overlapping 3-month periods at or above the +1.5ºC anomaly for warm (El Niño) events and at or below the -1.5ºC anomaly for cold (La Niña) events. The ENSO year in this study starts in September-October-November and ends in August-September-October for each year from 1981 to 2015. Subsequently, the crop yield of quinoa and potato was compared with strong El Niño years. This relationship was analysed using parametric two sample t-test as well as the non-parametric Wilcoxon rank sum test. In more detail, the two sample t-test and Wilcoxon rank sum compare two independent data samples, with the difference that the first compares samples that assume a normal distribution, and the second is a non-parametric test which is based on the ranking of empirical values (Wilks, 2006). The null hypothesis of the two sample t-test was that crop yields during El Niño and neutral/moderate years have equal means. The null hypothesis of the Wilcoxon rank sum test was the crop yield during El Niño and neutral/moderate years are samples from continuous distributions with equal medians. Both tests compute two-sided p-value. When the hypothesis is equal to 1, the null hypothesis is rejected at 5% significance level. And the null hypothesis is accepted when it is equal to zero.

3. Results and Discussion

3.1 Validation of satellite imagery using gauged data

Validation of the satellite rain data using empirical precipitation data from the weather stations was done for the 23 locations where gauge precipitation data were available (see Fig. 2 and Table A1). Interestingly, the spearman rank correlation between ground observed precipitation and satellite rain product datasets was significant ($P<0.001$) for all locations. The correlation coefficients were higher than 0.7, except for Colcha K [6] (brackets indicate the position of the station detailed in Table A1), that presented a significant ($P<0.001$) correlation of 0.66. Hence, the findings suggest that CHIRPS shows a significant positive relationship with empirical data. However, still the satellite datasets should be used with caution and its applicability for hydrological analysis applications tested. In addition, El Alto Aeropuerto [10], Oruro Aeropuerto [13], and Viacha [23] present the highest correlation coefficient with values higher than 0.9 ($P<0.001$). The datasets from the airports in Bolivia have higher data quality (e.g. Hunziker et al., 2018) and CHIRPS gives the best fits with the El Alto Aeropuerto [10] and Oruro Aeropuerto [13] for the statistical performance evaluation as described above, including the categorical tests mentioned. In summary, our results suggest a high degree of confidence in the CHIRPS performance compared to empirical data using the Spearman correlation coefficient as a performance measure. The ME (bias) between satellite and gauged data showed a range from -15 to 15% for most of the stations (Fig. 3a), representing a very good fit (Moriasi et al., 2007; Shrestha et al., 2017). However, the bias for Berenguela [4], Santiago de Machaca [20], and Viacha [23] was about 25%. Furthermore, the bias for Colcha K [6], Conchamarca [8], Hichucota [12], and San Juan Huancollo [17] was about -18%. The dataset for San Pablo de Lipez [18] had a bias of -29%. Previous studies indicate a bias from -25 to 25% representing a satisfactory fit (see Moriasi et al., 2007). Other studies have included a bias from -30 to 30% as satisfactory fit (see Shrestha et al., 2017). In conclusion, all datasets had acceptable bias.

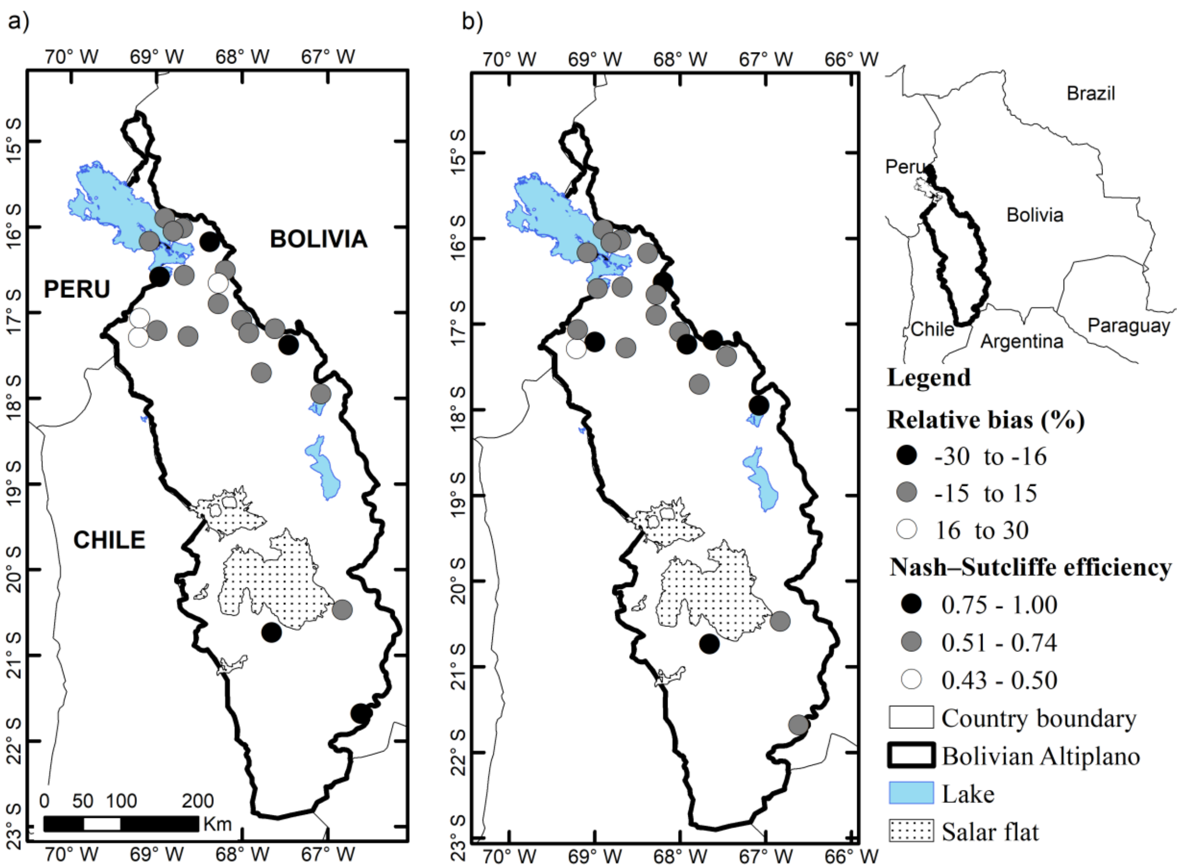

Fig. 3. (a) The relative mean error or bias (%) and (b) the Nash–Sutcliffe efficiency coefficient of the CHIRPS rain data compared with the gauged precipitation from September 1981 to August 2015.

The Nash–Sutcliffe efficiency coefficients (E) were larger than 0.5 for all stations except Berenguela [4] with a coefficient of 0.43 (Fig. 3b). As a consequence, the E coefficients showed that the mean square error is lower than the variance of the gauged data for all stations, including Berenguela. The E coefficients were larger than 0.75 for Achiri [1], Colcha K [6], El Alto Aeropuerto [10], Oruro Aeropuerto [13], Patacamaya [14], and Salla [15]. These datasets presented a very good fit between the CHIRPS and gauged precipitation, and the others also showed good fits, except for Berenguela [4] (see Moriasi et al., 2007).

The categorical statistics were used for a precipitation event (larger than 0 mm/month). The results of the Probability of Detection (POD) measure showed a range from 0.92 to 1, indicating that the satellite rain product correctly estimates above 0.92 for the fraction of gauged precipitation events. Additionally, the False Alarm Ratio (FAR) showed values from 0 to 0.3 for most stations, except Colcha K [6] and Uyuni [22] that had a FAR of about 0.5. Both stations are located in the southern Bolivian Altiplano, close to the Uyuni salt flat. CHIRPS generally overestimated rainfall with about 5 to 10 mm/month for both regions during the dry season (from April to October). Therefore, using a threshold of precipitation events larger than 10 mm/month resulted in a decrease of FAR to 0.2 and 0.3 for Colcha K [6] and Uyuni [22], respectively. Hence, in general the CHIRPS estimations presented a reasonably good fit compared to gauged data. The best fit was for the gauged datasets at the airports (El Alto Aeropuerto [10] and Oruro Aeropuerto [13]) that have better data quality, and consequently the validation showed better performance there. The datasets with a unsatisfactory fit included Colcha K [6] (with a correlation lower than 0.7) and Berenguela [4] (with an E lower than 0.5). The bias for San Pablo de Lipez [18] can be seen as acceptable depending of the ranking used. For the categorical analysis, all stations presented a good POD and FAR, except for Colcha K [6] and Uyuni [22] that tended to overestimate the precipitation during the dry season. In general, CHIRPS rainfall product properly estimated the actual conditions in the study area. However, for developing other hydrological studies we suggest to compare with the available gauged data before applying the CHIRPS datasets, in order to identify possible errors, and datasets with larger uncertainty or confidence.

Moving from rainfall to temperature, the inter-annual temperature at the 11 locations varied considerably between summer (DJFM) and winter (JJAS), including a larger variance for the minimum temperature (Fig. 1a). Regions close to the Lake Titicaca present lower inter-annual variability (Copacabana [9]). In contrast, Uyuni [22] showed larger inter-annual oscillations. The mean monthly temperature from satellite data was compared with mean temperature gauged data. The LST underestimated the mean gauged temperature, and this error could be due to the high elevation and cloud coverage. The spearman correlation at the 11 stations displayed coefficients from 0.8 to 0.9 (p=001). This permitted to correct the LST with linear regression. The regression results presented a range of coefficient of determination from 0.7 to 0.9 for all stations, meaning that the variability of gauged temperature is reasonably well explained by the LST. The results of linear regression approaches were applied to define the adjusted LST, that is the raw LST times 0.88 plus 5.7 degrees Celsius. The adjusted LST and the mean gauged temperature data showed acceptable relative bias (±25%) and E (≥0.5) coefficients for all stations. The same linear equation regression approach was used to correct the datasets of LST for all the studied area.

3.2 Regression of NDVI and climate variables

The precipitation season is occurs mainly during the austral summer months (DJFM), and the vegetation development shows a lag with a maximum development around March and April (Fig 1). The NDVI (Fig 1b) shows a similar growing pattern as the crop phenology in the region, which starts in September and ends in April. Also, the maximum and minimum temperature vary during the year. The latter shows even larger variability, with higher temperatures during the austral summer. And this could lead to higher evapotranspiration that might decrease the water retained in the root zone. With this presumption, we analysed the relationship between NDVI and climate variables. In a first step, the relationship between the maximum NDVI during the major phenological development months (i.e. March-April) and the corresponding annual crop yield between 1981 and 2015 was defined. A total of 26 and 76 NDVI grids estimated properly the quinoa and potato yield, respectively (Fig. 4). These are locations were NDVI showed a good correspondence with quinoa and potato yield, a correlation equal or larger than 0.6 (spearman correlation, p = 0.05) was used as a threshold for acceptable performance.

In a next step, stepwise linear regression models were tested using the selected NDVI grids and accumulated CHIRPS rainfall datasets at the same spatial location with a lag of two, three, and four months and which were found statistically significant at the 0.01 level. The coefficient of determination (R^2) oscillated from 0.4 to 0.7 in both cases. Additionally, stepwise linear regression for NDVI as independent variable, and the accumulated precipitation and ADD as dependant variables was performed (Eq. 1). The results also showed statistical significance for all locations included in the study. The R^2 oscillated from 0.5 to 0.8. It should be noted that the R^2 is generally larger in the northern and central Bolivian Altiplano, where the total precipitation is also larger. These are strong indications that precipitation and temperature explains the variability of the crop yield, and the influence is more notable in the northern and central Bolivian Altiplano. Figure 4 shows the coefficient of determination resulting from stepwise regression between NDVI, and precipitation, and temperature with a four-month lag.

Nat. Hazards Earth Syst. Sci. Discuss., https://doi.org/10.5194/nhess-2018-403
Manuscript under review for journal Nat. Hazards Earth Syst. Sci.
Discussion started: 27 March 2019

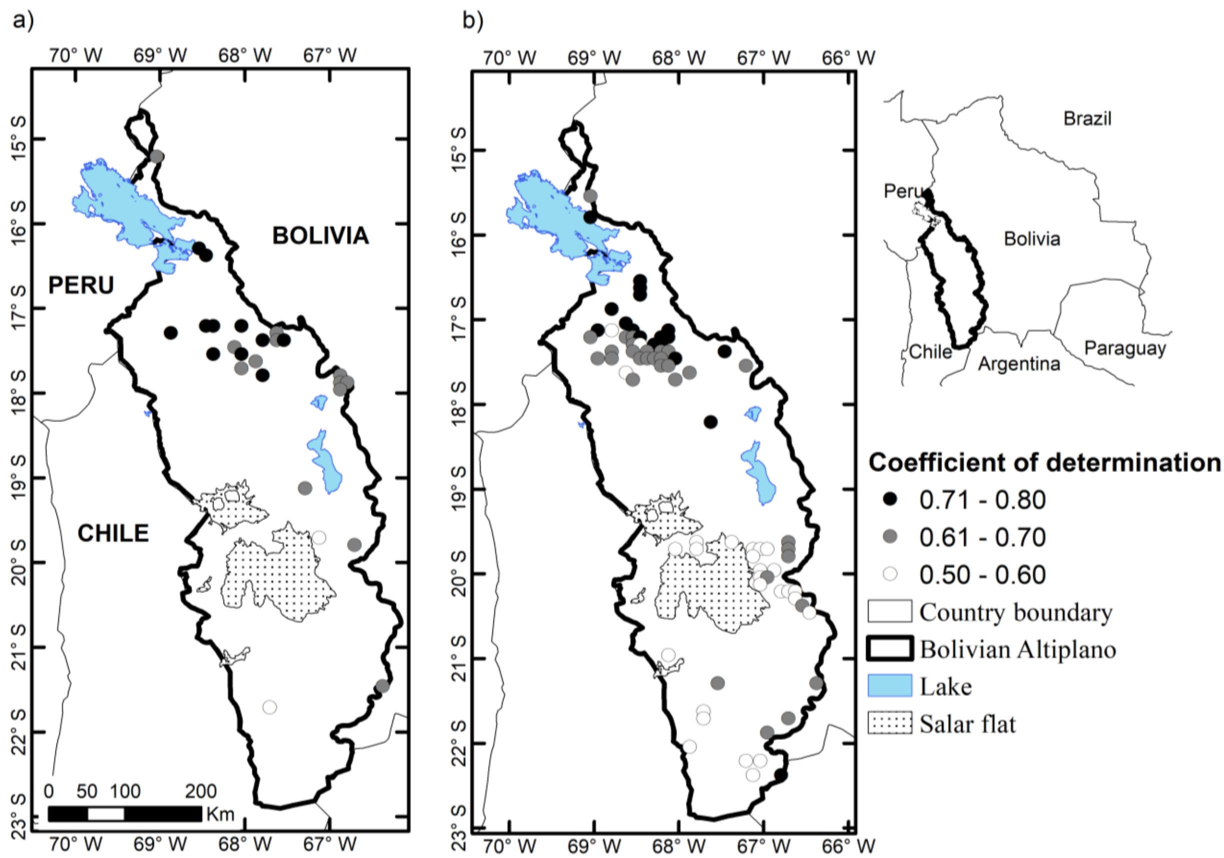

Fig. 4. The circles show the spatial location where NDVI properly estimates the (a) quinoa and (b) potato yield. And the graduated colours show the coefficient of determination (R^2) of the stepwise regression between NDVI as the predictand, and precipitation and temperature as the predictors with a lag of 4 months.

The regression models with only precipitation as dependent variable showed a larger coefficient of determination for three and four-month lag. In northern and central Bolivian Altiplano (16 to19 °LS) larger R^2 was found with a three-month lag and in the southern Bolivian Altiplano (20 to 22° LS) with a fourth-month lag. The results are related to different sowing time and starting period of the rainy season in the areas. In the northern Bolivian Altiplano the rainy season extends longer in time than in the southern Altiplano, where the rainy season is mainly concentrated to the austral summer months (DJF, Fig A1). Regression with precipitation and temperature as dependent variables showed larger coefficients of determination for a four-month lag. The hours of sun required for crop development could be the explanation for these results.

3.3 Relationship between ENSO and crop yield

After a reasonable relationship between NDVI and the satellite based climate datasets the next question to be tackled is relation to ENSO phases (as well as possible strategies to mitigate effects of these). As indicated, the relationship between ENSO and crop yield was analysed using two sample t-test and Wilcoxon Rank-Sum Tests for La Paz, Oruro, and Potosi (see Fig. 2c). To test the relationship, crop yield during neutral/moderate years was compared with crop yield during El Niño years (warm ENSO phase) (see Table A2). The results showed that quinoa yield during warm ENSO phase and neutral/moderate years presents a significant difference at 95% confidence level except for Oruro (Table A3). The yield during neutral/moderate years is higher with about 0.2 t/ha compared to El Niño years. The quinoa yield production during El Niño years is lower than the mean yield for neutral/moderate years, except for Oruro during 1982-1983 (Fig. 5). This finding contradicts previous studies that reported large agricultural losses during 1982-1983 and 1997-1998 (Santos, 2006). On the other hand, the quinoa yield has constantly increased during the last years, mainly in Oruro. This could be explained by employment of advanced crop management strategies (e.g., selected crop varieties and application of agricultural innovations), as this region is one of the largest producer in Bolivia and the world (Ormachea and Ramirez, 2013).

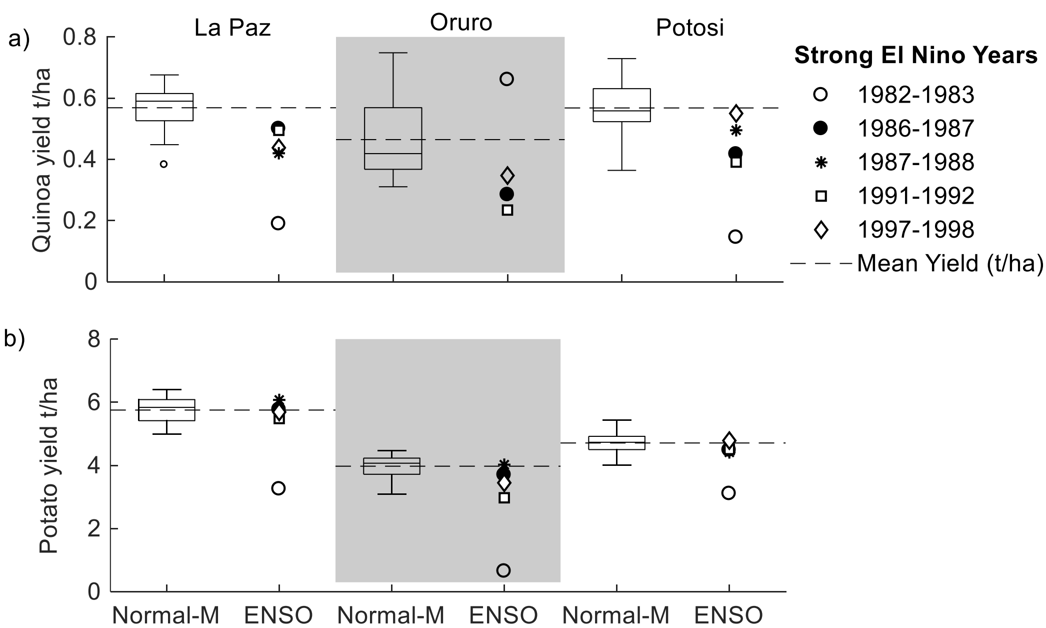

Fig 5. The boxplot of the (a) quinoa and (b) potato yield for normal and moderate years (Normal-M) for La Paz, Oruro, and Potosi. And the crop yield during strong El Nino years (markers). The mean of the crop yield during the normal and moderate years (dashed line).

Despite the quinoa's high tolerance to environmental stress including droughts (Jacobsen et al., 2005; Jacobsen et al., 2003), it generally showed larger losses during El Niño events than potato (Fig. 2). This may be due to the crop´s sensitivity for water stress during specific stages of the growing season, and the most sensitive stages are the emergence, flowering and grain development (see Geerts et al., 2009; Geerts et al., 2008a). The risk for crop yield reduction could be reduced here with irrigation during the sensitive phases of the quinoa crop development. A strategy like deficit irrigation could be employed (Talebnejad and Sepaskhah, 2015; Geerts et al., 2008b). Another strategy to mitigate the crop yield reduction is implementation of crop varieties more resistant to water stress (e.g. Sun et al., 2014).

The t-test and Rank-Sum test results showed that potato yield during neutral/moderate and El Niño years is significantly different at 95% confidence level except for La Paz (Table A3). The results showed that production during neutral/moderate years is higher in Oruro and Potosi. All regions showed lowest potato yield during strong El Niño for 1982-1983, with a yield reduction of 40, 80, and 30%, as compared to mean yield during normal/moderate years in La Paz Oruro and Potosi, respectively. The yield reduction during other El Niño events seems to have a larger effect in Oruro. Besides El Niño events during 1982-1983, potato yield in La Paz showed lower vulnerability to this phenomenon. This could be explained by closeness to the Lake Titicaca and other water bodies that might be used as a water source during precipitation deficit. Similar strategies for drought mitigation (e.g., irrigation and resistant crop varieties) could be implemented in order to avoid large crop losses. However, knowing that a very strong El Niño could lead to large agricultural losses, insurance policy could be assigned to farmers in order to manage the risk before the occurrence of a drought event. For the implementation of any drought mitigation strategy, identification, evaluation, and monitoring of drought risk are crucial. What is important is our findings that ENSO must be taken explicitly into account in such considerations.

4. Summary and conclusions

We employed a satellite dataset product and tested it for accuracy as well as performance to similar (but with coarser resolution) datasets available for our region. Using these datasets, it was shown that during El Niño years the crop yield reduces considerably (Figure 5 Table A3), and as a consequence the socio-economic vulnerability of farmers, will likely increase during such periods. Furthermore, it was found that NDVI can be related to crop yield and therefore, NDVI could be used to target specific hot spots depending on NDVIs availability at a local scale. As a consequence, ENSO forecasts as well as possible magnitudes of crop deficits could be established which may be beneficial for emergency authorities, including identification of possible hotspots of crop deficits during the growing season. Our approach can help to determine the magnitude of assistance needed for farmers at the local level but can also enable a pro-active approach to disaster risk management against droughts. This may include not only economic related instruments such as insurance but also risk reduction instruments such as irrigation and resistant crop varieties as discussed above. In fact, risk management based financing is gaining increasing attraction in real-world settings as it has several advantages. However, it should be acknowledged that large challenges still remain (French and Mechler, 2017).

The drought severity could be measured via time shifts from normal conditions of climatic parameters such as precipitation. As in our case, we not only elucidated shifts but also the difference in risk for El Niño and neutral/moderate years. However, one of the main challenges of drought risk analysis is data-scarcity, e.g., low density or unevenly distributed stations for hydro-meteorological data networks, poor data quality due to missing data, and restricted use of data between government agencies or other institutions. As it was shown here, ENSO warm phase related characteristics are especially important in the context of extreme drought events and should therefore be incorporated within early warning systems as standard practice. Despite these challenges for development of drought risk assessment, applications have been successful in the past. There are numerous cases in many countries and as in our case, particularly in the mid-latitudes where weather patterns are strongly influenced by ENSO. Monitoring and predicting ENSO can therefore significantly contribute to reduce the risk of disasters.

This study is a first attempt to provide an agricultural drought risk assessment in relation to the ENSO phenomenon for the Bolivian Altiplano. Our study provided valuable information for drought risk reduction, primarily by finding information of hotspots where crop yield is more affected by droughts and how this can be clarified using satellite imagery. However, while an overall good fit between climate, ENSO, and crop yield variables was found, it is important to consider other variables, such as evapotranspiration and soil moisture to improve risk-based models. With such information also agricultural models could be set up and risk management plans with better accuracy determined.

Acknowledgements

Part of this research was done during the Young Scientist Summer Program (YSSP) 2017 of the International Institute for Applied System Analysis (IIASA). This research was supported by FORMAS Research Council for Environment, Landscaping and Urban Development, and the Swedish International Development Cooperation Agency (SIDA). The authors would like to express their gratitude the Servicio Nacional de Meteorologia e

Hidrologia (SENAMHI) for providing the meteorological data. The authors would also like to thank Ramiro Pillco Zola and Angel Aliaga for the coordination of the research project with the Universidad Mayor de San Andres of Bolivia.

References

Anderson, W., Seager, R., Baethgen, W., and Cane, M.: Life cycles of agriculturally relevant ENSO teleconnections in North and South America, Int. J. Climatol., 37, 3297-3318, doi:10.1002/joc.4916, 2017.

Bartholmes, J. C., Thielen, J., Ramos, M. H., and Gentilini, S.: The european flood alert system EFAS – Part 2: Statistical skill assessment of probabilistic and deterministic operational forecasts, Hydrol. Earth Syst. Sci., 13, 141-153, 10.5194/hess-13-141-2009, 2009.

Beck, P. S. A., Atzberger, C., Høgda, K. A., Johansen, B., and Skidmore, A. K.: Improved monitoring of vegetation dynamics at very high latitudes: A new method using MODIS NDVI, Remote Sens. Environ., 100, 321-334, https://doi.org/10.1016/j.rse.2005.10.021, 2006.

Blacutt, L. A., Herdies, D. L., de Gonçalves, L. G. G., Vila, D. A., and Andrade, M.: Precipitation comparison for the CFSR, MERRA, TRMM3B42 and Combined Scheme datasets in Bolivia, Atmospheric Research, 163, 117-131, https://doi.org/10.1016/j.atmosres.2015.02.002, 2015.

Buxton, N., Escobar, M., Purkey, D., and Lima, N.: Water scarcity, climate change and Bolivia: Planning for climate uncertainties, Stockholm Environment Institute U.S. Center – Davis Office Davis, USA, 4, 2013.

Chuai, X. W., Huang, X. J., Wang, W. J., and Bao, G.: NDVI, temperature and precipitation changes and their relationships with different vegetation types during 1998–2007 in Inner Mongolia, China, Int. J. Climatol., 33, 1696-1706, doi:10.1002/joc.3543, 2013.

Condom, T., Rau, P., and Espinoza, J. C.: Correction of TRMM 3B43 monthly precipitation data over the mountainous areas of Peru during the period 1998–2007, Hydrol. Process., 25, 1924-1933, 10.1002/hyp.7949, 2011.

Cui, L., and Shi, J.: Temporal and spatial response of vegetation NDVI to temperature and precipitation in eastern China, Journal of Geographical Sciences, 20, 163-176, 10.1007/s11442-010-0163-4, 2010.

Duan, Y., Wilson, A. M., and Barros, A. P.: Scoping a field experiment: error diagnostics of TRMM precipitation radar estimates in complex terrain as a basis for IPHEx2014, Hydrol. Earth Syst. Sci., 19, 1501-1520, 10.5194/hess-19-1501-2015, 2015.

French, A., and Mechler, R.: Managing El Niño Risks Under Uncertainty in Peru: Learning from the past for a more disaster-resilient future, International Institute for Applied Systems Analysis, Laxenburg, Austria, 2017.

Funk, C., Peterson, P., Landsfeld, M., Pedreros, D., Verdin, J., Shukla, S., Husak, G., Rowland, J., Harrison, L., Hoell, A., and Michaelsen, J.: The climate hazards infrared precipitation with stations—a new environmental record for monitoring extremes, A Nature Research Journal, 2, 150066, 10.1038/sdata.2015.66, 2015.

Garcia, M., Raes, D., and Jacobsen, S.-E.: Evapotranspiration analysis and irrigation requirements of quinoa (Chenopodium quinoa) in the Bolivian highlands, Agric. Water Manage., 60, 119-134, https://doi.org/10.1016/S0378-3774(02)00162-2, 2003.

Garcia, M., Raes, D., Jacobsen, S. E., and Michel, T.: Agroclimatic constraints for rainfed agriculture in the Bolivian Altiplano, J Arid Environ., 71, 109-121, https://doi.org/10.1016/j.jaridenv.2007.02.005, 2007.

Garreaud, R. D., and Aceituno, P.: Interannual rainfall variability over the South American Altiplano, J. Clim., 14, 2779-2789, 10.1175/1520-0442(2001)014<2779:Irvots>2.0.Co;2, 2001.

Geerts, S., Raes, D., Garcia, M., Mendoza, J., and Huanca, R.: Crop water use indicators to quantify the flexible phenology of quinoa (Chenopodium quinoa Willd.) in response to drought stress, Field Crops Res., 108, 150-156, https://doi.org/10.1016/j.fcr.2008.04.008, 2008a.

Geerts, S., Raes, D., Garcia, M., Vacher, J., Mamani, R., Mendoza, J., Huanca, R., Morales, B., Miranda, R., Cusicanqui, J., and Taboada, C.: Introducing deficit irrigation to stabilize yields of quinoa (Chenopodium quinoa Willd.), Eur J Agron, 28, 427-436, https://doi.org/10.1016/j.eja.2007.11.008, 2008b.

Geerts, S., Raes, D., Garcia, M., Miranda, R., Cusicanqui, J. A., Taboada, C., Mendoza, J., Huanca, R., Mamani, A., Condori, O., Mamani, J., Morales, B., Osco, V., and Steduto, P.: Simulating Yield Response of Quinoa to Water Availability with AquaCrop, Agron. J., 101, 499-508, 10.2134/agronj2008.0137s, 2009.

Holben, B. N.: Characteristics of maximum-value composite images from temporal AVHRR data, Int J Remote Sens, 7, 1417-1434, 10.1080/01431168608948945, 1986.

Huang, J., Wang, H., Dai, Q., and Han, D.: Analysis of NDVI Data for Crop Identification and Yield Estimation, IEEE Journal of Selected Topics in Applied Earth Observations and Remote Sensing, 7, 4374-4384, 10.1109/JSTARS.2014.2334332, 2014.

Hunziker, S., Brönnimann, S., Calle, J., Moreno, I., Andrade, M., Ticona, L., Huerta, A., and Lavado-Casimiro, W.: Effects of undetected data quality issues on climatological analyses, Clim. Past, 14, 1-20, 10.5194/cp-14-1-2018, 2018.

Iizumi, T., Luo, J.-J., Challinor, A. J., Sakurai, G., Yokozawa, M., Sakuma, H., Brown, M. E., and Yamagata, T.: Impacts of El Niño Southern Oscillation on the global yields of major crops, Nature Communications, 5, 3712, 10.1038/ncomms4712 https://www.nature.com/articles/ncomms4712#supplementary-information, 2014.

IPCC: Climate Change 2013: The Physical Science Basis. Contribution of Working Group I to the Fifth Assessment Report of the Intergovernmental Panel on Climate Change, edited by: Stocker, T. F., Qin, D., Plattner, G.-K., Tignor, M., Allen, S. K., Boschung, J., Nauels, A., Xia, Y., Bex, V., and Midgley, G. F., Cambridge University Press, Cambridge, United Kingdom and New York, NY, USA, 1535 pp., 2013.

Jacobsen, S. E., and Bach, A. P.: The influence of temperature on seed germination rate in quinoa (Chenopodium quinoa Willd, Seed Science and Technology (Switzerland), 26, 515-523, 1998.

Jacobsen, S. E., Mujica, A., and Jensen, C. R.: The Resistance of Quinoa (Chenopodium quinoaWilld.) to Adverse Abiotic Factors, Food Rev. Int., 19, 99-109, 10.1081/FRI-120018872, 2003.

Jacobsen, S. E., Monteros, C., Christiansen, J. L., Bravo, L. A., Corcuera, L. J., and Mujica, A.: Plant responses of quinoa (Chenopodium quinoa Willd.) to frost at various phenological stages, Eur J Agron, 22, 131-139, https://doi.org/10.1016/j.eja.2004.01.003, 2005.

Ji, L., and Peters, A. J.: Assessing vegetation response to drought in the northern Great Plains using vegetation and drought indices, Remote Sens. Environ., 87, 85-98, https://doi.org/10.1016/S0034-4257(03)00174-3, 2003.

Kogan, F., and Guo, W.: Strong 2015–2016 El Niño and implication to global ecosystems from space data, Int J Remote Sens, 38, 161-178, 10.1080/01431161.2016.1259679, 2017.

Kutner, M. H., Nachtsheim, C., and Neter, J.: Applied linear regression models, McGraw-Hill/Irwin, 2004.

Moriasi, D. N., Arnold, J. G., Van Liew, M. W., Bingner, R. L., Harmel, R. D., and Veith, T. L.: Model Evaluation Guidelines for Systematic Quantification of Accuracy in Watershed Simulations, Transactions of the ASABE, 50, 885-900, https://doi.org/10.13031/2013.23153, 2007.

Nash, J. E., and Sutcliffe, J. V.: River flow forecasting through conceptual models part I — A discussion of principles, J. Hydrol., 10, 282-290, https://doi.org/10.1016/0022-1694(70)90255-6, 1970.

Ochoa, A., Pineda, L., Crespo, P., and Willems, P.: Evaluation of TRMM 3B42 precipitation estimates and WRF retrospective precipitation simulation over the Pacific–Andean region of Ecuador and Peru, Hydrol. Earth Syst. Sci., 18, 3179-3193, 10.5194/hess-18-3179-2014, 2014.

Ormachea, E., and Ramirez, N.: Propiedad colectiva de la tierra y producción agrícola capitalista: El caso de la quinua en el Altiplano Sur de Bolivia, first ed., Centro de Estudios para el Desarrollo Laboral y Agrario (CEDLA),

Bolivia, 208 pp., 2013.
Ramirez-Rodrigues, M. A., Asseng, S., Fraisse, C., Stefanova, L., and Eisenkolbi, A.: Tailoring wheat management to ENSO phases for increased wheat production in Paraguay, Climate Risk Management, 3, 24-38, https://doi.org/10.1016/j.crm.2014.06.001, 2014.
Rencher, A. C.: Methods of Multivariate Analysis, John Wiley & Sons, New York, 1995.
Santos, J. L.: The Impact of El Niño - Southern Oscillation Events on South America, Adv. Geosci., 6, 221-225, 2006.
Satgé, F., Bonnet, M.-P., Gosset, M., Molina, J., Hernan Yuque Lima, W., Pillco Zolá, R., Timouk, F., and Garnier, J.: Assessment of satellite rainfall products over the Andean plateau, Atmospheric Research, 167, 1-14, 10.1016/j.atmosres.2015.07.012, 2016.
Shinoda, M.: Seasonal phase lag between rainfall and vegetation activity in tropical Africa as revealed by NOAA satellite data, Int. J. Climatol., 15, 639-656, 10.1002/joc.3370150605, 1995.
Shrestha, N. K., Qamer, F. M., Pedreros, D., Murthy, M. S. R., Wahid, S. M., and Shrestha, M.: Evaluating the accuracy of Climate Hazard Group (CHG) satellite rainfall estimates for precipitation based drought monitoring in Koshi basin, Nepal, Journal of Hydrology: Regional Studies, 13, 138-151, https://doi.org/10.1016/j.ejrh.2017.08.004, 2017.
Sun, Y., Liu, F., Bendevis, M., Shabala, S., and Jacobsen, S.-E.: Sensitivity of Two Quinoa (ChenopodiumquinoaWilld.) Varieties to Progressive Drought Stress, Journal of Agronomy and Crop Science, 200, 12-23, doi:10.1111/jac.12042, 2014.
Talebnejad, R., and Sepaskhah, A. R.: Effect of deficit irrigation and different saline groundwater depths on yield and water productivity of quinoa, Agric. Water Manage., 159, 225-238, https://doi.org/10.1016/j.agwat.2015.06.005, 2015.
Thompson, L. G., Mosley-Thompson, E., and Arnao, B. M.: El Niño-Southern Oscillation events recorded in the stratigraphy of the tropical Quelccaya ice cap, Peru, Science, 226, 50-53, 10.1126/science.226.4670.50, 1984.
Tippett, M. K., Barnston, A. G., and Li, S.: Performance of Recent Multimodel ENSO Forecasts, J. Appl. Meteorol. Clim., 51, 637-654, 10.1175/jamc-d-11-093.1, 2012.
UN: The Sustainable Development Goals Report 2016, United Nations New York, USA, 2016.
UNISDR: Drought Risk Reduction Framework and Practices: Contributing to the Implementation of the Hyogo Framework for Action, United Nations secretariat of the International Strategy for Disaster Reduction (UNISDR), Geneva, Switzerland, 2009.
UNISDR: Making Development Sustainable: The Future of Disaster Risk Management. Global Assessment Report on Disaster Risk Reduction, United Nations Office for Disaster Risk Reduction (UNISDR), Geneva, Switzerland, 266, 2015.
Verbist, K., Amani, A., Mishra, A., and Cisneros, B. J.: Strengthening drought risk management and policy: UNESCO International Hydrological Programme's case studies from Africa and Latin America and the Caribbean, Water Policy, 18, 245-261, 10.2166/wp.2016.223, 2016.
Vicente-Serrano, S. M., Chura, O., López-Moreno, J. I., Azorin-Molina, C., Sanchez-Lorenzo, A., Aguilar, E., Moran-Tejeda, E., Trujillo, F., Martínez, R., and Nieto, J. J.: Spatio-temporal variability of droughts in Bolivia: 1955–2012, Int. J. Climatol., 35, 3024-3040, 10.1002/joc.4190, 2015.
Wilks, D. S.: Statistical Methods in the Atmospheric Sciences, second ed., Academic Press, 2006.
Zhou, C., and Wang, K.: Land surface temperature over global deserts: Means, variability, and trends, J. Geophys. Res. Atmos., 121, 14,344-314,357, doi:10.1002/2016JD025410, 2016.

Nat. Hazards Earth Syst. Sci. Discuss., https://doi.org/10.5194/nhess-2018-403
Manuscript under review for journal Nat. Hazards Earth Syst. Sci.
Discussion started: 27 March 2019

Natural Hazards and Earth System Sciences
Open Access
Discussions

APPENDIX

Table A1. Spatial location of the studied weather stations where gauged precipitation data is available, the stations that also present temperature maximum and minimum data indicate T on the column of temperature.

N_o	Station name	Region	Latitude	Longitude	Altitude	Temperature
[1]	Achiri	La Paz	-17.21	-69.00	3880	T
[2]	Ancoraimes	La Paz	-15.90	-68.90	3882	
[3]	Ayo Ayo	La Paz	-17.09	-68.01	3888	T
[4]	Berenguela	La Paz	-17.29	-69.21	4145	
[5]	Calacoto	La Paz	-17.28	-68.64	3830	T
[6]	Colcha K	Potosí	-20.74	-67.66	3780	
[7]	Collana	La Paz	-16.90	-68.28	3911	T
[8]	Conchamarca	La Paz	-17.38	-67.46	3965	
[9]	Copacabana	La Paz	-16.17	-69.09	3870	
[10]	El Alto Aeropuerto	La Paz	-16.51	-68.20	4034	T
[11]	El Belen	La Paz	-16.02	-68.70	3833	
[12]	Hichucota	La Paz	-16.18	-68.38	4460	
[13]	Oruro Aeropuerto	Oruro	-17.95	-67.08	3701	T
[14]	Patacamaya	La Paz	-17.24	-67.92	3793	T
[15]	Salla	La Paz	-17.19	-67.62	3500	
[16]	San Jose Alto	La Paz	-17.70	-67.78	3746	T
[17]	San Juan Huancollo	La Paz	-16.58	-68.96	3829	
[18]	San Pablo de Lipez	Potosí	-21.68	-66.61	4256	
[19]	Santiago de Huata	La Paz	-16.05	-68.81	3845	
[20]	Santiago de Machaca	La Paz	-17.07	-69.20	3883	
[21]	Tiahuanacu	La Paz	-16.57	-68.68	3863	T
[22]	Uyuni	Potosí	-20.47	-66.83	3680	T
[23]	Viacha	La Paz	-16.66	-68.28	3850	T

Table A2. The classification of strong El Niño (≥ 1.5 deg C), strong La Niña (≤ -1.5 dec C) and neutral/moderate (-1.4 to 1.4 dec C) years for the period 1981 to 2015.

Strong El Niño	Neutral and moderate	Strong La Niña
1982-83	1981	1988-89
1986-87	1984-1985	1998-99
1987-88	1989-1990	2007-08
1991-92	1992-1996	2010-11
1997-98	2000-2006	
	2008-2009	
	2011-2014	

Nat. Hazards Earth Syst. Sci. Discuss., https://doi.org/10.5194/nhess-2018-403
Manuscript under review for journal Nat. Hazards Earth Syst. Sci.
Discussion started: 27 March 2019

Table A3. T-test and Wilcoxon rank sum test for quinoa and potato yield during El Niño years and neutral/moderate years. If the hypothesis is equal to 1 it means that we rejected the null hypothesis at a confidence level of 95%.

		T test 2 sample			Wilcoxon rank sum test		
		Hypothesis	P value	t-stat	Hypothesis	P value	z-stat
Quinoa	La Paz	1	~0	4.2	1	0.01	3.0
	Oruro	0	0.13	1.6	1	0.05	2.0
	Potosi	1	~0	3.4	1	0.04	2.5
Potato	La Paz	0	0.10	1.7	0	0.54	0.61
	Oruro	1	~0	3.4	1	0.02	2.4
	Potosi	1	0.02	2.6	1	0.05	2.0

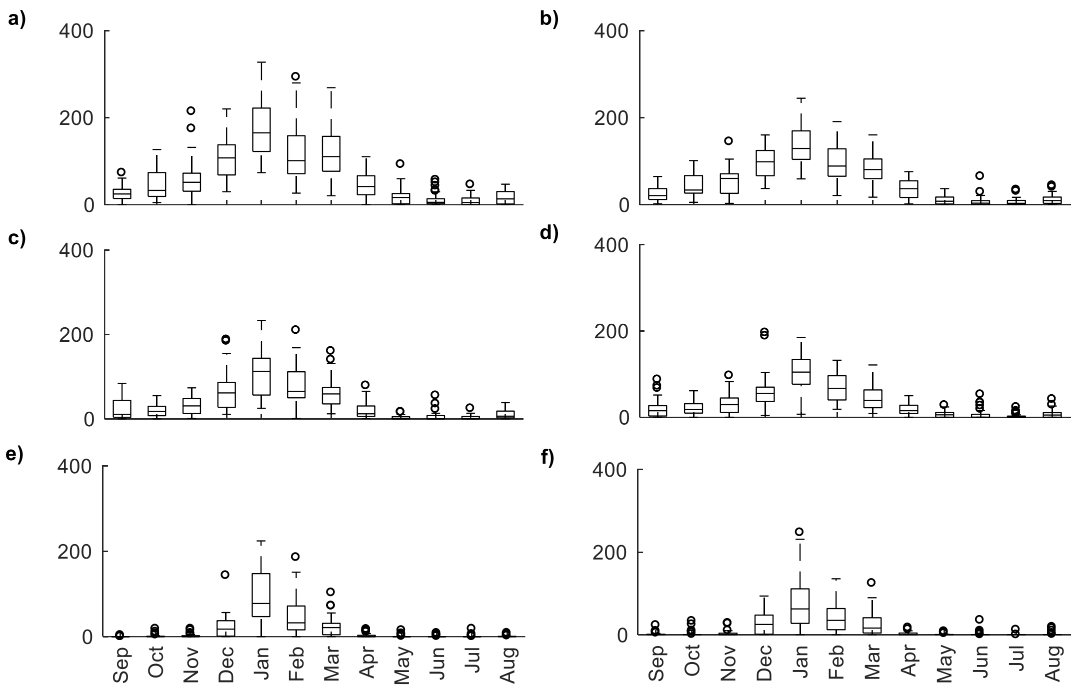

5 **Figure A1.** Boxplot of the total monthly precipitation in the Bolivian Altiplano at the northern Altiplano: (a) Copacabana [9], (b) El Alto Aeropuerto [10], central Altiplano: (c) Oruro Aeropuerto [13], (d) Patacamaya [14], and southern Altiplano (e) Colcha K [6], and (f) Uyuni [22].